Phosphorylation and Mutation of Human Cardiac Troponin I Deferentially Destabilize the Interaction of the Functional Regions of Troponin I with Troponin C[†,‡]

Monica X. Li,[§] Xu Wang,[§] Darrin A. Lindhout,[§] Nina Buscemi,[#] Jennifer E. Van Eyk,[#] and Brian D. Sykes*[,§]

CIHR Group in Protein Structure and Function, Department of Biochemistry, University of Alberta, Edmonton, Alberta, Canada T6G 2H7, and Department of Physiology, Queen's University, Kingston, Ontario K7L 3N6

Received August 7, 2003; Revised Manuscript Received October 1, 2003

ABSTRACT: We have utilized 2D {^{1}H,^{15}N}-HSQC NMR spectroscopy to elucidate the binding of three segments of cTnI in native, phosphorylated, and mutated states to cTnC. The near N-terminal region (cRp; residues 34−71) contains the protein kinase C (PKC) phosphorylation sites S41 and S43, the inhibitory region (cIp; residues 128−147) contains another PKC site T142 and a familial hypertrophic cardiomyopathy (FHC) mutation R144G, and the switch region (cSp; residues 147−163) contains the novel p21-activated kinase (PAK) site S149 and another FHC mutation R161W. While S41/S43 phosphorylation of cRp had minimal disruption in the interaction of cRp and cTnC·3Ca^{2+}, T142 phosphorylation reduced the affinity of cIp for cCTnC·2Ca^{2+} by ∼14-fold and S149 phosphorylation reduced the affinity of cSp for cNTnC·Ca^{2+} by ∼10-fold. The mutation R144G caused a ∼6-fold affinity decrease of cIp for cCTnC·2Ca^{2+} and mutation R161W destabilized the interaction of cSp and cNTnC·Ca^{2+} by ∼1.4-fold. When cIp was both T142 phosphorylated and R144G mutated, its affinity for cCTnC·2Ca^{2+} was reduced ∼19-fold, and when cSp was both S149 phosphorylated and R161W mutated, its affinity for cNTnC·Ca^{2+} was reduced ∼4-fold. Thus, while the FHC mutation R144G enhances the effect of T142 phosphorylation on the interaction of cIp and cCTnC·2Ca^{2+}, the FHC mutation R161W suppresses the effect of S149 phosphorylation on the interaction of cSp and cNTnC·Ca^{2+}, demonstrating linkages between the FHC mutation and phosphorylation of cTnI. The observed alterations corroborate well with structural data. These results suggest that while the modifications in the cRp region have minimal influence, those in the key functional cIp-cSp region have a pronounced effect on the interaction of cTnI and cTnC, which may correlate with the altered myofilament function and cardiac muscle contraction under pathophysiological conditions.

The myofilament is the contractile machinery in cardiac myocytes and plays a vital role in maintaining the normal function of heart. Activation of myofilament is controlled through the contractile proteins, which include a heterotrimeric troponin complex (cTnC, cTnI, and cTnT),[1] tropomyosin, actin, and myosin. During diastole, troponin holds tropomyosin in a conformational state that blocks the interaction between myosin and actin. When Ca^{2+} binds cTnC during systole, the troponin−tropomyosin complex moves from its blocking position facilitating interaction of thick filament myosin heads with the thin filament and generation of ATPase activity and muscle contraction. Sequestration of Ca^{2+} by the sarcoplasma reticulum reverses the process with ensuing diastolic relaxation (for reviews, see refs *1* and *2*).

As key components of this system, the functional and structural relationships of cTnC and cTnI and their interactions in the presence and absence of Ca^{2+} have been the subject of intensive investigation. The solution structure of the Ca^{2+}-saturated cTnC has revealed a dumbbell molecule with two globular domains connected by a flexible linker (*3*) and this flexibility is decreased in the presence of cTnI (*4*). The solution structures of the N-domain of cTnC in both

[†] Supported by the Canadian Institutes of Health Research (CIHR) and the Heart and Stroke Foundation of Canada. X.W. is supported by both a CIHR studentship and an Alberta Heritage Foundation for Medical Research Studentship and D.A.L. is supported by an Alberta Heritage Foundation for Medical Research Studentship.

[‡] Note: S41, S43, T142, R144, S149, and R161 in recombinant human cTnI correspond to S42, S44, T143, R145, S150, and R162, respectively, in the wild-type protein, which has an extra N-terminal Met residue. In this article, the sequence numbering of cTnI follows that of recombinant cTnI.

* To whom correspondence should be addressed. Phone: (780) 492−5460. Fax: (780) 492−0886. E-mail: brian.sykes@ualberta.ca.

[§] Department of Biochemistry, University of Alberta.

[#] Queen's University.

[1] Abbreviations: TnC, troponin C; cTnC, cardiac muscle TnC; sTnC, skeletal muscle TnC; cNTnC, N-domain (1−89) of cTnC with mutations C35S and C84S; cCTnC, C-domain (91−161) of cTnC; TnI, troponin I; cTnI, cardiac muscle TnI; sTnI, skeletal muscle TnI; cRp, synthetic peptide Ac-cTnI$_{34-71}$-NH$_2$; cRp-S41P/S43P, synthetic peptide Ac-cTnI$_{34-71}$-NH$_2$ with S41 and S43 phosphorylated; cSp, synthetic peptide Ac-cTnI$_{147-163}$-NH$_2$; cSp-S149P, synthetic peptide Ac-cTnI$_{147-163}$-NH$_2$ with S149 phosphorylated; cSp-R161W, synthetic peptide Ac-cTnI$_{147-163}$-NH$_2$ with mutation R161W; cSp-S149P-R161W, synthetic peptide Ac-cTnI$_{147-163}$-NH$_2$ with S149 phosphorylated and mutation R161W; cIp, synthetic peptide Ac-cTnI$_{128-147}$-NH$_2$, cIp-T142P, synthetic peptide Ac-cTnI$_{128-147}$-NH$_2$ with T142 phosphorylated; cIp-R144G, recombinant peptide NH$_3^+$-cTnI$_{128-147}$-hSer-CO$_2^-$ with mutation R144G; cIp-T142P-R144G, synthetic peptide Ac-cTnI$_{128-147}$-NH$_2$ with T142 phosphorylated and mutation R144G.

10.1021/bi035408y CCC: $25.00
Published on Web 11/15/2003

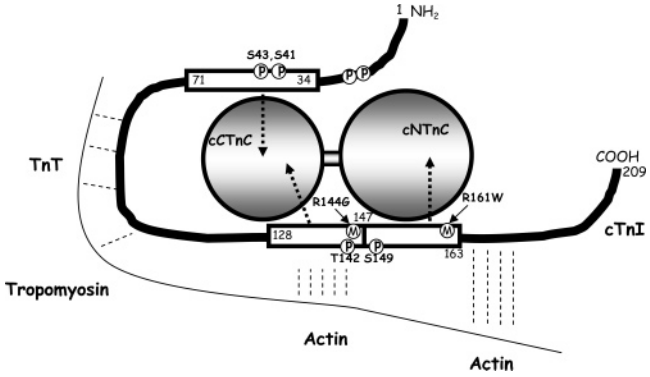

FIGURE 1: A schematic representation of the interaction of cTnC with cTnI with the cRp, cIp, and cSp regions, the phosphorylation sites, and mutation sites indicated.

the apo and Ca^{2+}-bound states have defined the Ca^{2+}-induced conformational transition in the regulatory domain of cTnC (*5*). Using the structure of cTnC as a framework, biochemical and biophysical studies have clarified how various regions of cTnI react with cTnC and participate in thin filament Ca^{2+}-signaling (see Figure 1 and for a review, see ref *6*). These involve the near N-terminal segment of cTnI (cRp; ~ residues 34−71), the inhibitory region (cIp; ~ residues 128−147), and the switch region (cSp; ~ residues 147−163). While high affinity interaction between cTnC and cRp likely persists throughout the systolic−diastolic cycle, weaker Ca^{2+}-dependent interactions permit cIp-cSp toggling between cTnC and actin−tropomyosin. The high-resolution structure of cTnC−cTnI complexes includes the X-ray structure of $sTnC{\cdot}2Ca^{2+}{\cdot}sTnI_{1-47}$ (*7*), the NMR structures of $cNTnC{\cdot}Ca^{2+}{\cdot}cSp$ (*8*) and $cCTnC{\cdot}2Ca^{2+}{\cdot}cIp$ (*9*), and the 2.6 Å X-ray structure of $cTnC{\cdot}3Ca^{2+}{\cdot}cTnI_{31-210}{\cdot}cTnT_{183-288}$ (*10*). These structures have demonstrated that cRp interacts extensively with the C-domain of cTnC, cIp primarily interacts with the C-domain of cTnC, and cSp is directly responsible for binding to the N-domain of cTnC and stabilizing the open conformation of $cNTnC{\cdot}Ca^{2+}$.

cTnI and cTnI−cTnC interactions are subject to modifications by intracellular signaling molecules, which play vital roles in mediating the myofilament activation. Phosphorylation of cTnI appears to be of particular importance in modulating myofilament activity. Two serine residues (S22 and S23) that are substrates for protein kinase A (PKA) lie within the N-terminal extension of cTnI (for a review, see ref *6*). cTnI is also sensitive to protein kinase C (PKC) phosphorylation at S41, S43, and T142. The effect of cTnI phosphorylation by those kinases is primarily a downward modulation of cardiac contractility, either by decreased actomyosin ATPase activity, which is mediated by PKC, or by enhanced Ca^{2+} dissociation from cTnC and reduced myofilament Ca^{2+} sensitivity, mediated by PKA. Recently, a study has shown that p21-activated kinase (PAK) increases the Ca^{2+}-sensitivity of Triton-skinned cardiac muscle fiber bundles via a mechanism potentially involving the phosphorylation of cTnI at S149 (*11*), representing a novel cTnI phosphorylation site in addition to the PKA and PKC sites.

cTnI mutation is also implicated in various cardiac diseases. For example, familial hypertrophic cardiomyopathy (FHC), one of the most frequently occurring inherited cardiac disorders, has been identified to be a sarcomere disease (for reviews, see refs *12* and *13*) and is believed to be caused by mutations in certain contractile protein genes, including cTnI. To date, six FHC mutations [R144G, R144Q, R161W, S198N, G202S, and K207Q][‡] on cTnI have been reported along with mutations causing the deletion of one codon (K182) and a deletion of exon 8 (Δexon8) (*13*). Among those, R144G and R144Q are located in the key inhibitory region and R161W is located in the important switch region of cTnI. A truncation of cTnI has been associated with myocardial stunning (*14*, *15*), and measuring the serum level of cTnI has become the standard of care in the diagnosis of myocardial injury (*16*−*19*).

To understand how alterations in cTnI are involved in disease, it is important to elucidate the effects of cTnI modifications on its interaction with cTnC. Although many functional and animal model experiments have revealed the functional differences between native and modified cTnI that may underline the pathogenesis of cardiac disease (*15*, *20*−*25*), there are little data available concerning the structural consequences of cTnI modification with regard to the interaction of cTnI with cTnC or cTnI with actin−tropomyosin, especially on the combined effects of FHC mutation with phosphorylation of cTnI. In this study, we have utilized 2D $\{^1H,^{15}N\}$-HSQC NMR spectroscopy to elucidate the binding of three segments (cRp, cIp, and cSp) of cTnI in native, S41, S43, and T142 phosphorylated, and R144G and R161W mutated states to cTnC. While S41/S43 phosphorylation of cRp had minimal disruption in the interaction of cRp and $cTnC{\cdot}3Ca^{2+}$, the affinity of cIp for $cCTnC{\cdot}2Ca^{2+}$ and cSp for $cNTnC{\cdot}Ca^{2+}$ was reduced by the modifications in all cases. An important and novel finding of this work was that while the FHC mutation R144G enhances the effect of T142 phosphorylation on the interaction of cIp and $cCTnC{\cdot}2Ca^{2+}$, the FHC mutation R161W suppresses the effect of S149 phosphorylation on the interaction of cSp and $cNTnC{\cdot}Ca^{2+}$, demonstrating linkages between FHC mutation and phosphorylation of cTnI. The observed alterations corroborate well with the structural data. The results suggest that while the modifications in the cRp region have minimal influence those in the key functional cTnI region (cIp and cSp) have a pronounced effect on the interaction of cTnI and cTnC, which may correlate with the altered myofilament function and cardiac muscle contraction under pathophysiological conditions.

EXPERIMENTAL PROCEDURES

Protein Sample Preparation. In this work, recombinant human cTnC(1−161) and cNTnC(1−89) with the mutations C35S and C84S were used. The engineering of the expression vector of cTnC(C35S/C84S) and cNTnC(C35S/C84S) was as described elsewhere (*26*, *27*). For the purpose of clarity, (C35S/C84S) is omitted in the following sections. The engineering of the expression vector for the cCTnC(91−161) protein was as described previously (*28*). Protocols for transformation, expression in BL21 (DE3) *pLysS* cells and purification of ^{15}N-cTnC, ^{15}N-cNTnC, and ^{15}N-cCTnC were as described in a previous publication (*29*). Two NMR samples of ^{15}N-$cTnC{\cdot}3Ca^{2+}$ were prepared for the titrations of cRp and cRp-S41P/S43P, four NMR samples of ^{15}N-$cNTnC{\cdot}Ca^{2+}$ were prepared for the titrations of cSp, cSp-S149P, cSp-R161W, and cSp-S149P-R161W, and four NMR samples of ^{15}N-$cCTnC{\cdot}2Ca^{2+}$ were prepared for the titrations of cIp, cIp-T142P, cIp-R144G, and cIp-T142P-R44G. Stan-

dard NMR buffer [100 mM KCl, 10 mM imidazole, 0.2 mM 2,2-dimethyl-2-silapentanesulfonic acid (DSS), and 0.01% NaN_3 in 90% H_2O/10% D_2O] was used in all cases. The sample concentrations were determined by amino acid analysis. To each sample was added 5 μL of 1 M $CaCl_2$ to ensure that the protein was Ca^{2+}-saturated, and the pH was adjusted to 6.7 by 1 M HCl and/or 1 M NaOH.

Synthetic Peptides. acetyl-AKKKSKI**S**A**S**RKLQLKTLLLQIAKQELEREAEERRGEK-amide (cRp), acetyl-RI**S**ADAMMQALLGARAK-amide (cSp), acetyl-RI**S**ADAMMQALLGAWAK-amide (cSp-R161W), acetyl-TQKIFDLRGKFKRP**T**LRRVR-amide (cIp), and acetyl-TQKIFDLRGKFKRP**T**LGRVR-amide (cIp-R144G) were prepared using standard methodology for a typical TnI peptide (*30*). Standard methodology was also used to synthesize cRp-S41P/S43P, cSp-S149P, cSp-S149P-R161W, cIp-T142P, and cIp-T142P-R144G except that phosphorylated amino acid (bold and underlined in the sequences) is incorporated. The sequences were confirmed by amino acid analysis, and the mass was verified by electrospray mass spectrometry.

Construction and Expression of cIp-R144G Peptide. The construct of the recombinant cIp-R144G peptide was produced as follows: the DNA region encoding residues 128−147 of human cTnI was obtained using primer 1 5′-CTAGCATGACCCAGAAAATTTTTGATCTGCGCGGCAAATTTAAACGCCCGACCCTGGGCCGCGTGCGCATGCCCGGGC-3′ and primer 2 5′-TCGAGCCCGGGCATGCGCACGCGGCCCAGGGTCGGGCGTTTAAATTTGCCGCGCAGATCAAAAATTTTCTGGGTCATG-3′. Subsequent ligation with GEV-1 vector (*31*), expression, and purification of cIp-R144G are as previously described for cIp-R145G (*32*).

Titration of ^{15}N-cTnC·3Ca^{2+} with cRp and cRp-S41P/S43P. Both cRp and cRp-S41P/S43P peptides are highly soluble in water, which allows the preparation of a 35 mM stock solution of cRp and a 40 mM stock solution of cRp-S41P/S43P. A 500 μL NMR sample of 0.6 mM ^{15}N-cTnC·3Ca^{2+} was used for the titration with cRp and a 500 μL NMR sample of 0.7 mM ^{15}N-cTnC·3Ca^{2+} was used for the titration with cRp-S41P/S43P. Each titration was done by adding consecutive aliquots of 1 μL of cRp or cRp-S41P/S43P stock solutions. The sample was mixed thoroughly with each addition. The change in protein concentration due to dilution was taken into account for data analysis. The decrease in pH associated with cRp or cRp-S41P/S43P addition was adjusted by 1 M NaOH to pH 6.7 at every titration point. Both 1D ^{1}H and 2D {^{1}H, ^{15}N}-HSQC NMR spectra were acquired at every titration point.

Titration of ^{15}N-cNTnC·Ca^{2+} with cSp, cSp-S149P, cSp-R161W, and cSp-S149P-R161W. cSp peptide is slightly soluble in aqueous solution and tends to form a gel at high concentrations (>50 mM), likely due to aggregation. Thus, no stock peptide solution was prepared; instead, solid peptide was added directly to the NMR tube at every titration point. A 500 μL 0.6 mM sample of ^{15}N-cNTnC·Ca^{2+} was used for the cSp titration, a 500 μL 0.5 mM sample was used for the cSp-S149P titration, a 500 μL 0.7 mM sample was used for the cSp-R161W titration, and a 500 μL 0.6 mM sample was used for the cSp-S149P-R161W titration. The sample was mixed thoroughly with each addition. Two microliters of sample in duplicate was taken at every titration point for amino acid analysis to determine the peptide/protein ratios. Changes in pH associated with cSp additions were compensated by adjusting to pH 6.7 at every titration point. Both 1D ^{1}H and 2D {^{1}H, ^{15}N}-HSQC NMR spectra were acquired at every titration point.

Titration of ^{15}N-cCTnC·2Ca^{2+} with cIp, cIp-T142P, cIp-R144G, and cIp-T142P-R144G. The titration of ^{15}N-cCTnC·2Ca^{2+} with cIp and cIp-T142P were done as described previously (*32*). Stock solutions of recombinant cIp-R144G (41 mM) and synthetic cIp-T142P-R144G (49 mM) in NMR buffer were prepared and used for two separate titrations. (i) To a NMR tube containing a 500 μL sample of 0.92 mM ^{15}N-cCTnC·2Ca^{2+} were added aliquots of 1 μL of 41 mM cIp-R144G for the first 10 titration points. Aliquots of 2 μL were added for the next four titration points, followed by consecutive addition of 4, 10, 25, and 40 μL for the last four titration points. (ii) To a NMR tube containing a 500 μL sample of 0.49 mM ^{15}N-cCTnC·2Ca^{2+} were added aliquots of 1 μL of 49 mM cIp-T142P−R144G for the first 6 titration points. Aliquots of 1.5, 1.5, 2, and 2 μL were added consecutively for the next four titration points, followed by consecutive addition of 3, 4, 10, and 10 μL for the last four titration points. At each titration point, 1 μL of sample was taken for amino acid analysis. The change in protein concentrations due to increased volume during the titration was taken into account for data analysis. The change in pH from cIp-R144G or cIp-T142P-R144G additions was negligible. Both 1D ^{1}H and 2D {^{1}H, ^{15}N}-HSQC spectra were acquired at every titration point.

NMR Spectroscopy. All of the NMR spectra were obtained using a Unity INOVA 500 MHz spectrometer at 30 °C. All 1D ^{1}H NMR spectra were acquired with a sweep width of 6000 or 7000 Hz with 128 transients. All 2D {^{1}H, ^{15}N}-HSQC spectra were acquired using the sensitivity-enhanced gradient pulse scheme developed by Lewis E. Kay and coworkers (*33*, *34*). The ^{1}H and ^{15}N sweep widths were 6000 or 7000 Hz and 1500 Hz, with 16 transients and 128 increments, respectively. Spectral processing and analyses were accomplished with the program VNMR (Varian Associates), NMRPipe (*35*), and NMRView (*36*).

RESULTS

Effect of S41/S43 Phosphorylation on the Interaction of cRp with cTnC·3Ca^{2+}. Previously, we have shown that cRp binds cCTnC·2Ca^{2+} in a 1:1 stoichiometry to form a tight cCTnC·2Ca^{2+}·cRp complex ($K_D \leq 1$ μM) and the interaction of cRp with cCTnC·2Ca^{2+} occurs with slow exchange kinetics on the NMR time scale (*37*). A similar binding behavior of cRp for cTnC·3Ca^{2+} indicates that the interaction of this region of cTnI binds specifically to the C-domain of cTnC·3Ca^{2+} regardless of the presence of the N-domain (*27*). Here we compare the binding behavior of cRp and cRp-S41P/S43P. Figure 2A shows a superimposition of an expanded region of the 2D {^{1}H, ^{15}N}-HSQC NMR spectra of cTnC·3Ca^{2+} and cTnC·3Ca^{2+}·cRp complex, and Figure 2B shows a superimposition of an expanded region of the 2D {^{1}H, ^{15}N}-HSQC NMR spectra of cTnC·3Ca^{2+} and cTnC·3Ca^{2+}·cRp-S41P/S43P complex. The 2D {^{1}H, ^{15}N}-HSQC NMR spectrum of cTnC·3Ca^{2+} is completely assigned (*3*) and is used as a guide in assigning some of the residues in the cRp or cRp-S41P/S43P bound states. In both cases, the C-domain residues underwent significant changes and several C-domain residues including G110 and G146 are

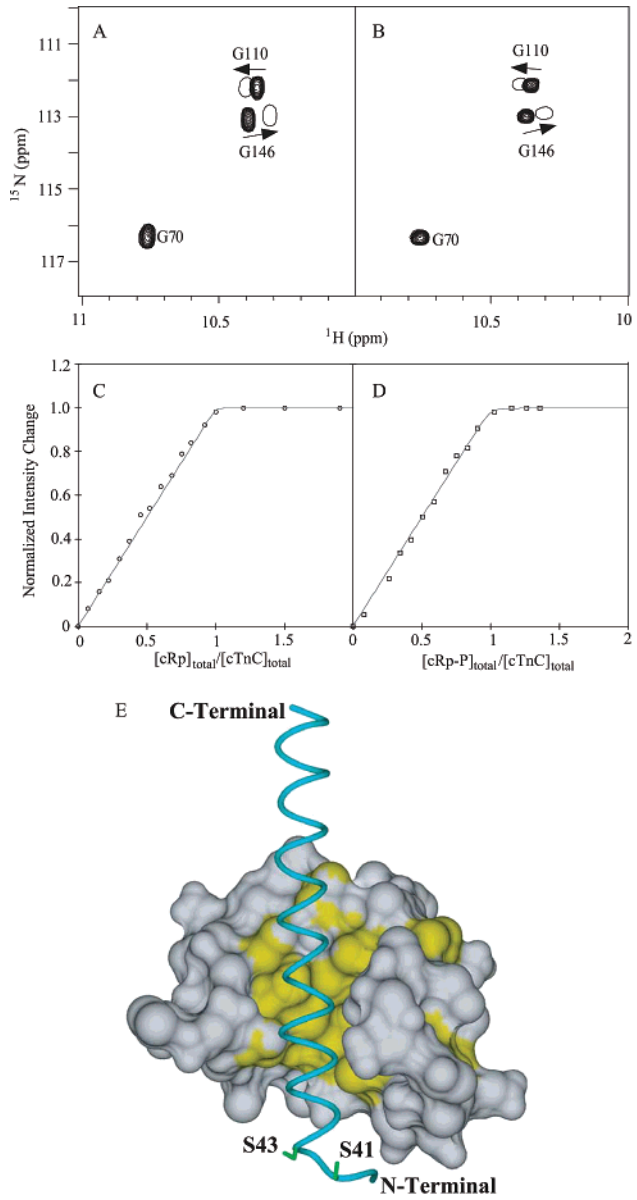

FIGURE 2: Titration of ^{15}N-cTnC·3Ca^{2+} with cRp (A) and cRp-S41P/S43P (B). In the expanded contour plots of the 2D {^{1}H, ^{15}N}-HSQC spectra, the cross-peaks corresponding to free cTnC·3Ca^{2+} are shown as multiple contours, whereas the peaks corresponding to the protein/peptide complexes are shown as single contours. The titration curves for cRp and cRp-S41P/S43P binding are shown in (C) and (D), respectively. Each curve is normalized according to $(I_{obs} - I_{initial})/(I_{final} - I_{initial})$, where I represents the cross-peak intensity changes. A solid line represents the best fit to the data. (E) Ribbon and surface representations of the structure of cCTnC·2Ca^{2+}·cRp in the cTnC·3Ca^{2+}·cTnI$_{31-210}$·cTnT$_{183-288}$ complex (PDB accession code 1J1E) (*10*). The positions of S41 and S43 phosphoylation sites are indicated.

labeled in Figure 2A,B as examples. As the titration progresses, the resonance peaks corresponding to cTnC·3Ca^{2+} becomes less intense, while those corresponding to the cTnC·3Ca^{2+}·cRp or cTnC·3Ca^{2+}·cRp-S41P/S43P complex grow. When the protein/peptide ratio reaches 1:1, all cross-peaks corresponding to cTnC·3Ca^{2+} have completely disappeared, while those corresponding to the complex attain maximum intensity. When the intensity changes as a function of peptide-to-protein ratios were plotted, the curve levels off after the protein/peptide ratio reaches 1:1. Figure 2C,D shows the respective binding curves of cRp and cRp-S41P/S43P for cTnC·3Ca^{2+}. In both cases, curve fitting yielded a dissociation constant $K_D \leq 1$ μM. It is important to point out that since the K_D values of ≤ 1 μM are far less than the concentrations of protein used in the NMR experiments, the affinity less than 1 μM becomes difficult to determine from a titration curve, i.e., it is hard to distinguish between K_D's of 1, 0.1, and 0.01 μM. Thus, our result indicates that the phosphorylation of S41/S43 did not destabilize the tight association of cRp with cTnC·3Ca^{2+} as the K_D is still equal or below 1 μM (indicative of high affinity between ligand and protein). Recent structural data on cRp−cTnC interaction are from the X-ray structure of the cTnC·3Ca^{2+}·cTnI$_{31-210}$·cTnT$_{183-288}$ complex (*10*), which shows that the cRp region forms a long α-helix interacting primarily with the C-domain of cTnC·3Ca^{2+} via multiple polar and van der Waals interactions, similar to the earlier structure of sTnC·2Ca^{2+}·sTnI$_{1-47}$ (*7*). As shown in Figure 2E, the α-helix enters the C-domain of cTnC hydrophobic cleft near helices G/H and exits near helices E/F and the S41/S43 phosphorylation sites are located approximately in the beginning of the α-helix with almost no direct contacts with the protein hydrophobic cleft. Thus, it is unlikely that the introduction of two negative charged phosphate groups at S41P/S43P would exert much influence on the extensive contacts between the long α-helix of cRp and the C-domain of cTnC. Interestingly, in both the sTnC·2Ca^{2+}·sTnI$_{1-47}$ and cTnC·3Ca^{2+}·cTnI$_{31-210}$·cTnT$_{183-288}$ structures, TnC adopts a collapsed conformation as such the N-terminus of the cRp α-helix makes several weak contacts with the N-lobe of cTnC. This is reflected in our observation that some of the N-domain peaks (e.g., G42, V72, V79) underwent slight chemical shift changes in the titration of cRp-S41P/S43P to cTnC·3Ca^{2+} (data not shown). It is possible that the two negative charged phosphate groups at S41P/S43P caused minor conformational alterations in the N-domain of cTnC.

Effect of S149 Phosphorylation and R161W Mutation on the Interaction of cSp with cNTnC·Ca^{2+}. Some of the resonance peaks in the 2D {^{1}H, ^{15}N}-HSQC spectrum of ^{15}N-cNTnC(C35S/C84S)·Ca^{2+} were assigned based on the assignments of wild type ^{15}N-cNTnC·Ca^{2+} (*5*). The complete assignments were achieved using CBCA(CO)NNH and HNCACB experiments (*38*) analyzed with the automated assignment program smartnotebook (*39*). The 2D {^{1}H, ^{15}N}-HSQC NMR spectrum of cNTnC·Ca^{2+} was used as a starting point to monitor the cSp peptides induced chemical shift changes. The cSp-induced 2D {^{1}H, ^{15}N}-HSQC NMR spectral change of ^{15}N-cNTnC·Ca^{2+} is very similar to that reported previously (*8*). The titrations of ^{15}N-cNTnC·Ca^{2+} with cSp-S149P, cSp-R161W, and cSp-S149P-R161W, respectively, are shown in Figure 3A. Comparison of the 2D {^{1}H, ^{15}N}-HSQC NMR spectral changes induced by the four cSp peptides reveal that all four peptides induce a similar pattern of backbone amide resonance changes of cNTnC·Ca^{2+}. Typical examples are G30, G34, and G42. In all cases, chemical shift changes fall into the fast exchange limit on the NMR time scale and the linear movement of the resonance peaks indicates that the binding occurs with a 1:1 stoichiometry.

Resonances which undergo backbone amide ^{1}H$_N$ and/or ^{15}N chemical shift changes during titrations were followed to monitor peptide binding to protein. For each titration, the peptide induced chemical shift changes of individual amide

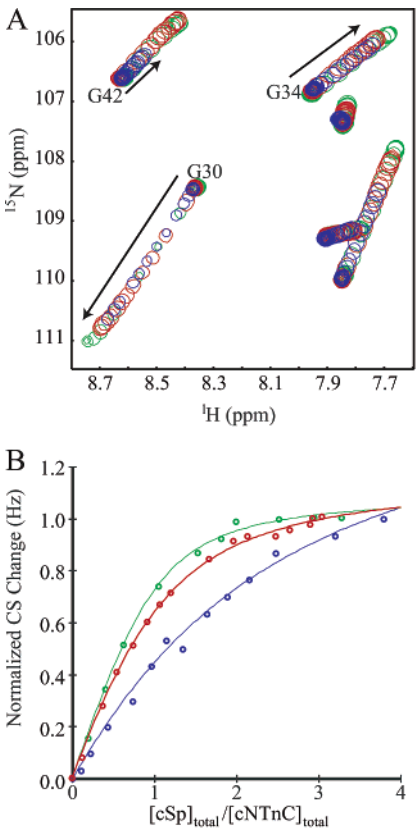

FIGURE 3: Titration of ^{15}N-cNTnC·Ca^{2+} with cSp-S149P (blue), cSp-R161W (green), and cSp-S149P-R161W (red). (A) Expanded regions of the 2D {^{1}H, ^{15}N}-HSQC NMR spectra of cNTnC·Ca^{2+} (●) at various peptide additions are superimposed (○), showing the progressive shifts of peaks with increasing peptide concentrations. (B) Titration curves representing the average of all residues followed in panel A. The curves are normalized according to $(\delta_{obs} - \delta_{initial})/(\delta_{complex} - \delta_{initial})$. A solid line represents the best fit to the data.

resonance as a function of the peptide/protein ratio was plotted, and the average curves (except for cSp, which is very similar to that published previously; *8*) are shown in Figure 3B. The curve fitting yielded a dissociation constants (K_D) of 130 ± 20 μM for cSp, 1.25 ± 0.2 mM for cSp-S149P, 176 ± 33 μM for cSp-R161W, and 394 ± 32 μM for cSp-S149P−R161W. This corresponds to an affinity reduction of ∼10-fold by the S149 phosphorylation, ∼1.4-fold by the mutation R161W, and ∼4-fold by a combination of S149 phosphorylation and mutation R161W.

To compare the four cSp peptides induced chemical shift changes of cNTnC, the normalized values for amide $^{1}H_N$ and ^{15}N were averaged and plotted against the protein sequence with different colors coding four cTnI peptides (Figure 4A). The important point of this plot is that the patterns induced by four peptides are very similar although to a slightly different extent. Although most of the residues throughout the sequence are more or less affected by peptides binding, 26 residues undergo significant ($\Delta\delta_{ppm} \geq 1.5$) peptide-induced chemical shift perturbations. Mapping those residues on the structure of cNTnC in the cNTnC·Ca^{2+}·cSp complex (Figure 4B) reveals that the peptide-induced chemical shift perturbations arise primarily from the A, B, and C-helices and the β-sheet regions. This is not surprising considering that these regions are directly involved in binding cSp and undergo large conformational changes in the cSp-induced "closed" to "open" structural transition of cNTnC. The fact that these residues are identical in all four cases indicates that neither the S149 phosphorylation, the mutation R161W, nor the combination of both, abolish the ability of cSp to induce a "closed" to "open" structural transition in cNTnC·Ca^{2+}. It is important to point out that when the 26 residues were mapped to the surface of cNTnC in the cNTnC·Ca^{2+}·cSp complex, it did not reveal a binding patch matching the hydrophobic surface as shown in Figure 4C. This is probably because the major conformational perturbation caused by cSp is on the "closed" to "open" structural transition, but not on the binding surface of cNTnC.

In the high-resolution structure of the cNTnC·Ca^{2+}·cSp complex (*8*), the α-helical segment (residues 151−156) of the 17-residue cSp peptide inserts between the A/B interhelical interface and the N-terminus (residues 147−149) interacts with the hydrophobic core of cNTnC and S149 is located in the center of the core (Figure 4C). As such two negative charges introduced by S149 phosphorylation would be expected to disrupt the hydrophobic force and lead to weaker binding of cSp for cNTnC·Ca^{2+} as observed in the current study. It is interesting to note that the affinity of cSp for cNTnC·Ca^{2+} is also weakened by the presence of bepridil in the hydrophobic core although to a smaller extent (∼3.5-fold reduction in affinity) (*40*). This indicates that the hydrophobic interaction is the primary anchoring force for cSp binding to cNTnC and stabilizing its opening conformation and it is easily disturbed by the introduction of a negatively charged phosphate group or a partially positively charged agent, such as bepridil. On the other hand, mutation R161W involves a basic to hydrophobic charge change and can be postulated to result an energetically more favorable interaction of the tryptophan side chain with the hydrophobic patch on cNTnC. Unfortunately, in the structure of the cNTnC·Ca^{2+}·cSp complex, the C-terminal residues (A160, R161, A162, and K163) of cSp do not interact with cNTnC·Ca^{2+} and extends out of the protein surface (Figure 4C). Thus, the mutation R161W may only have minimal effect on the interaction of cSp and cNTnC·Ca^{2+} as reflected in the observed ∼1.4-fold affinity decrease. The subtle affinity alteration observed herein is in accordance with a recent surface plasmon resonance-based (SPR) study showing that the affinity of R161W mutant for cTnC is only ∼2.6 times that of wild-type cTnI (*20*). Somewhat surprisingly, the effect of S149 phosphorylation is compromised in the presence of R161W mutation, i.e., a ∼4-fold affinity decrease by cSp-S149P-R161W as compared to a ∼10-fold one by cSp-S149P. It is possible that the ∼10-fold weakening caused by the phosphorylation of S149 allows the tryptophan side chain of R161W rearrange its position slightly so it makes an energetically more favorable interaction with cNTnC·Ca^{2+} and therefore increasing the apparent affinity. At present, there is no compelling data for rationalization.

Effect of T142 Phosphorylation and R144G Mutation on the Interaction of cIp with cCTnC·2Ca^{2+}. Previously, we have utilized 2D {^{1}H, ^{15}N}-HSQC NMR spectroscopy to monitor the binding of cIp and cIp-T142P to cCTnC·2Ca^{2+} (*32*). The dissociation constants determined were 31 ± 11 μM for cIp and 451 ± 10 μM for cIp-T142P, indicating a ∼14-fold affinity reduction by the phosphorylation of T142. In the present work, we examined the influence of FHC mutation R144G on the interaction of cIp or cIp-T142P with

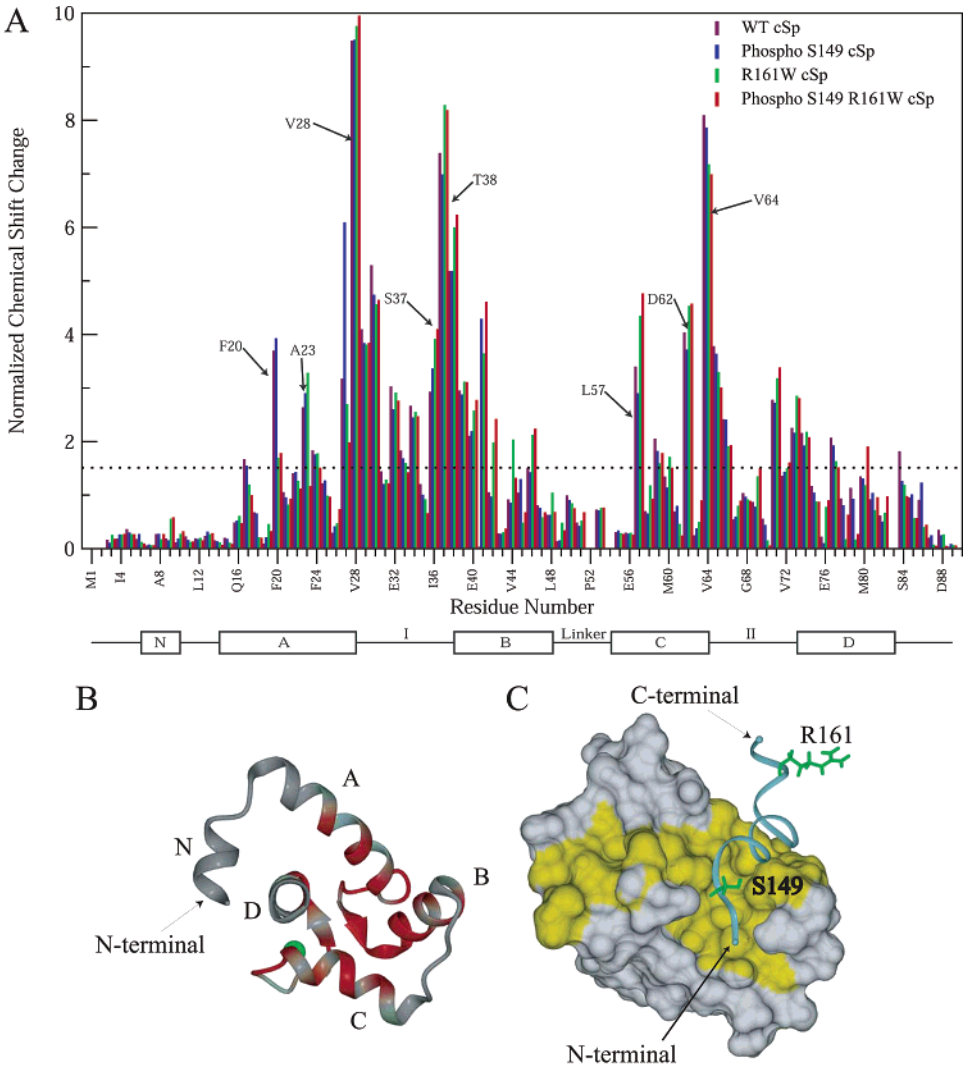

FIGURE 4: (A) Comparison of induced chemical shift changes of cNTnC·Ca^{2+} upon the addition of cSp (maroon), cSp-S149P (blue), cSp-R161W (green), and cSp-S149P-161W (red). The chemical shift changes for each residue were calculated by averaging the normalized chemical shift changes of the backbone $^{1}H_N$ and ^{15}N chemical shifts. For a particular nucleus, the normalized chemical shift change of a residue is obtained by dividing the observed shift change by the average shift change for all residues. Thus, $\Delta\delta_{ppm} = 1$ indicates that the chemical shift change for a given residue is equal to the average change for all residues. (B) Chemical shift mapping on the structure of cNTnC in the cNTnC·Ca^{2+}·cSp complex (PDB accession code 1MXL) (*8*): the residues experience major chemical shift changes ($\Delta\delta_{ppm} \geq 1.5$) are colored red. (C) Residues S149 and R161 are shown on the structure of cNTnC·Ca^{2+}·cSp. The molecular surface of cNTnC·Ca^{2+} (residues 5−84) in the complex is shown with the hydrophobic surface colored yellow, the structure of cSp is shown in the "rods" representation.

cCTnC·$2Ca^{2+}$. The cIp-R144G or cIp-T142P-R144G induced 2D {^{1}H, ^{15}N}-HSQC NMR spectral changes are shown in Figure 5A. The patterns in the two titrations are similar, which are also similar to those observed in the titration of cCTnC·$2Ca^{2+}$ with cIp or cIp-T142P (*32*). Using the same approaches as for analyzing the binding of cIp and cIp-T142P, we plotted the cIp-R144G or cIp-T142P-R144G induced chemical shift changes of individual amide resonances as a function of the protein:peptide ratio and the average curves are shown in Figure 5B. Curve fitting yielded a dissociation constant (K_D) of 192 ± 21 μM for cIp-R144G and 581 ± 12 μM for cIp-T142P-R144G, corresponding to a ~6-fold affinity reduction by cIp-R144G and a ~19-fold reduction by cIp-T142P-R144G. Taken together, these results show that both T142P and R144G destabilize the binding of cIp for cCTnC·$2Ca^{2+}$ and the effect from both is cumulative. The plot of amide $^{1}H_N$ and ^{15}N chemical shift changes against the cCTnC sequence for cIp-R144G and cIp-T142P-R144G are analogous (data not shown) to those of cIp and cIp-T142P, indicating that either modification affects the binding epitope of cIp on the surface of cCTnC·$2Ca^{2+}$.

In the recent published NMR structure of cCTnC·$2Ca^{2+}$·cIp complex (*9*), residues L134−K139 of cIp forms a helix and residues R140−R147 adopts an extended conformation (Figure 5C). With the helical region interacting with the E and H helices of cCTnC, the highly basic R140−R147 region containing R140, R144, R145, and R147 makes potential electrostatic contacts with the acidic residues present on the linker region (beginning of the E-helix) including E94, E95, and E96. As phosphorylation of T142 introduces two negative charges and mutation R144G neutralizes the positive charged arginine side chain, both modifications make cIp less basic and therefore weaken the electrostatic interaction between cIp and cCTnC. Since T142P is in much closer proximity to the binding center of cIp on cCTnC·$2Ca^{2+}$ than R144G, a larger reduction in affinity by T142P is observed.

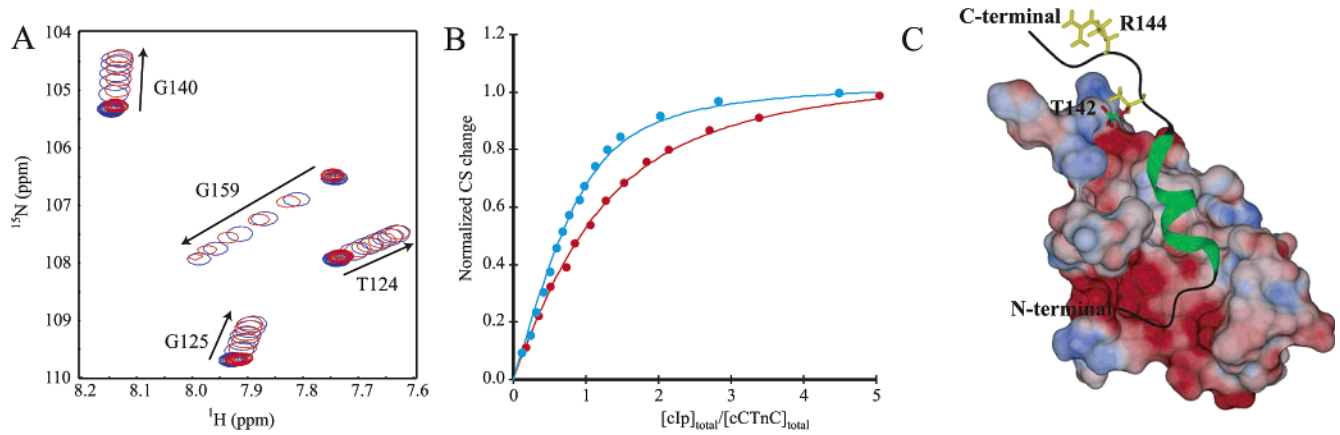

FIGURE 5: Titration of ^{15}N-cCTnC·2Ca^{2+} with cIp-R144G and cIp-T142P-R144G. (A) An expanded region of the 2D {^{1}H, ^{15}N}-HSQC NMR spectra of cCTnC·2Ca^{2+} (●) at various cIp-R144G (blue) and cIp-T142P-144G (red) additions are superimposed (○), showing the progressive shifts of peaks with increasing peptide concentrations. (B) Titration curves for the binding of cIp-R144G (blue) and cIp-T142P-144G (red) to cCTnC·2Ca^{2+}. The curve is normalized according to $(\delta_{obs} - \delta_{initial})/(\delta_{complex} - \delta_{initial})$. A solid line represents the best fit to the data. (C) Ribbon and surface representations of the structure of the cCTnC·2Ca^{2+}·cIp complex (PDB accession code 1OZS) (*9*). Residues T142 and R144 are labeled to indicate the sites of phosphorylation and mutation.

Table 1: K_D's (μM) for Peptides Binding to cTnC

	cTnC·3Ca^{2+}	cNTnC·Ca^{2+}	cCTnC·2Ca^{2+}
cRp	≤1		
cRp-S41P/S43P	≤1		
cSp		130 ± 20	
cSp-S149P		1250 ± 200	
cSp-R161W		176 ± 33	
cSp-S149P-R161W		394 ± 32	
cIp[a]			31 ± 11
cIp-T142P[a]			451 ± 10
cIp-R144G			192 ± 21
cIp-T142P-R144G			581 ± 12

[a] Data from Lindhout et al. (*32*).

This is also in line with our earlier result (*32*) that shows mutation R145G, which is further away than R144G, reduces the affinity of cIp for cCTnC·2Ca^{2+} by ~4-fold, as compared to a ~6-fold by R144G and ~14-fold by T142P. The structural analysis above also explains the current observation that shows the effect of T142 phosphorylation and mutation R144G is cumulative.

DISCUSSION

This study is directed toward an evaluation of the consequences caused by the phosphorylation of S41, S43, T142, and S149 and FHC mutations R144G and R161W on the interaction of cTnI with cTnC. We have utilized 2D {^{1}H, ^{15}N}-HSQC NMR spectroscopy as a tool to monitor and compare the chemical shift and spectral intensity changes in cTnC·3Ca^{2+} caused by cRp in native or modified states, in cNTnC·Ca^{2+} caused by cSp in native or modified states, and in cCTnC·2Ca^{2+} caused by cIp in native or modified states. This allows us to systematically assess the influences of these alterations on the binding location, stoichiometry, and affinity of three key regions of cTnI to cTnC. The binding constants for cRp peptides binding cTnC·3Ca^{2+}, cSp peptides binding to cNTnC·Ca^{2+}, and cIp peptides binding to cCTnC·2Ca^{2+} are summarized in Table 1.

Three specific PKC phosphorylation sites on cTnI have been identified at residues S41, S43, and T142. Although S41/S43 are sequentially distant from T142, the three sites are in close proximity upon binding cTnC·3Ca^{2+} as both cRp and cIp interact with the C-lobe of cTnC. Thus, it is not surprising that all three sites are phosphorylated upon the activation of PKC in cardiac myocytes. The relative contribution of the phosphorylation of three sites to the accelerated relaxation and decreased acto-myosin ATPase activity has been the focus of several recent studies. For example, Burkart et al. reported that phosphorylation of S41/S43 dominates regulation of the level of maximum tension, while phosphorylation of T142 appears to be required for regulation of thin filament sliding speed (*25*). The data presented here demonstrated that it is the phosphorylation of T142 but not S41/S43 that plays a major role in destabilizing the cTnI−cTnC interaction, which leads to diminished acto-myosin ATPase activity and depressed contractility. Since S41/S43 are located in the structural domain of the troponin complex based on the recent proposed model (*10*), the phosphorylation of S41/S43 may be involved in the global conformational changes of troponin in the thin filament rather than in the cTnI−cTnC interface. Residue S149 in the cSp region has been recently identified to be the site of p21-activated kinase (PAK), a kinase potentially involved in Ca^{2+}-sensitization of cardiac muscle contraction and cardiac hypertrophy. Current study has demonstrated that S149 phosphorylation reduced the affinity of cSp for cNTnC·Ca^{2+} by ~10-fold. Since S149 of cTnI is located in the center of the hydrophobic core of cNTnC·Ca^{2+} (*8*), introduction of a negatively charged phosphate group in this region of cTnI would certainly destabilize its binding to cNTnC·Ca^{2+} and result in reduced affinities. Given that the phosphorylation of S149 in cTnI may be involved in a mechanism of Ca^{2+}-sensitization of Triton-skinned cardiac muscle fiber (*11*) and considering that cTnI toggles between cTnC and actin-tropomyosin during the systolic−diastolic cycle, these results suggest a greater reduction in affinity of S149 phosphorylated cTnI for actin-tropomyosin as compared to cTnC. Thus cTnI−cTnC interactions would be favored compared to cTnI−actin−tropomyosin interaction resulting in an increase of the Ca^{2+}-affinity for cTnC and thereby the Ca^{2+}-sensitization of the myofilaments. Nonetheless, the dramatic affinity reduction of cTnI for cTnC by the phosphorylation

of either T142 or S149 strongly suggests that kinases such as PKC or PAK modulate cardiac muscle contraction by modifying myofilament protein−protein interaction, contributing to depressed contractility in certain cases and compromised relaxation in other.

In addition to phosphorylation, the cIp-cSp region of cTnI is also prone to missense mutations in diseased heart. Three mutations (R144G, R144Q, and R161W)[‡] that cosegregate with FHC are located in this highly conserved region (*13*). Both the R144G and R161W mutations constitute a change in charge and the latter involves the introduction of a large aromatic side chain. The functional abnormalities revealed reduced ability of R144G and R161W mutants to inhibit actomyosin ATPase and an increase in Ca^{2+} sensitivity of actomyosin ATPase regulation (*20*−*24*). If these functional differences manifest themselves in vivo there will be impairment of relaxation of cardiac muscle and this altered contractility may provide a hypertrophic stimulus eventually leading to cardiac dysfunction. This is supported by a mouse model study that shows that at the whole organ level, contractile function is enhanced but relaxation is compromised in mouse harboring the R144G mutation (*21*). Because cTnI toggles between cTnC and actin−tropomyosin, it seems likely that an important mechanism of cTnI-induced cardiac dysfunction by the R144G and R161W mutations lies in altered cTnI interactions with cTnC, actin−tropomyosin or both. The binding of cTnI to actin−tropomyosin inhibits actomyosin ATPase activity, depresses cross-bridge cycling, and prevents contraction. The inhibition is released as cTnI binding shifts from actin−tropomyosin to cTnC, an action favored by an increase in cytosolic Ca^{2+} concentration during systole, when Ca^{2+} binds to the N-domain of cTnC. Thus, it seems that the R144G or R161W mutated cTnI either has reduced affinity for actin−tropomyosin or enhanced affinity for cTnC. The net effect would be the diminished inhibition of actomyosin ATPase activity. Interestingly, our present results indicate that the affinity of cIp for cCTnC·$2Ca^{2+}$ is reduced by ∼6-fold by the mutation R144G and that of cSp for cNTnC·Ca^{2+} is reduced ∼1.4-fold by the mutation R161W. In light of the above argument, these results suggest a greater reduction in affinity of R144G and R161W mutants for actin-tropomyosin compared to cTnC, such that cTnI-cTnC interaction is favored over cTnI−actin−tropomyosin interaction, similar as in the case of S149 phosphorylation.

The fact that the cIp and cSp segments of cTnI are subject to modifications by both phosphorylation and mutation prompted us to examine the binding of cIp-T142P-R144G to cCTnC·$2Ca^{2+}$ and that of cSp-S149P-R161W to cNTnC·Ca^{2+}. The results show that T142P and R144G modifications have a cumulative effect on reducing the affinity of cIp for cCTnC·$2Ca^{2+}$; however, the destabilizing factor introduced by S149 phosphorylation on the interaction of cSp and cNTnC·Ca^{2+} is compromised somehow by the R161W mutation. Thus, it seems that the FHC mutations can either enhance or suppress the effect of phosphorylation depending on the specificity of the interactions. So far there is limited functional data available from literature linking the FHC mutations with cTnI phosphorylation. One study has compared the in vitro function of R144G mutation in nonphosphorylated and S22/S23 (PKA sites) bisphosphorylated cTnI and revealed that S22P/S23P and R144G exhibit mutual suppressing effect on the acto-myosin ATPase activity (*23*). Current data will be helpful for future work in understanding the mechanism of cTnI function involving both FHC mutations and PKC or PAK phosphorylation.

In summary, we have employed a very feasible system by the use of cTnI peptides to examine the consequences of cTnI modification on its interaction with cTnC. The results indicate that a given modification of cTnI can have a pronounced effect on the binding affinity of cTnI for cTnC. These perturbations in protein affinity may correlate with the impairment of cTnI function in heart muscle contraction. Clearly, further studies by employing the intact cTnI protein, the entire troponin complex, and even the entire thin filament are needed to generate a more complete picture in the understanding of the mechanism by which myofilament protein modifications promote cardiac dysfunction.

ACKNOWLEDGMENT

We thank Dr. L. B. Smillie for providing the cTnC(C35S/C84S) and cNTnC(C35S/C84S) constructs, Mr. D. Corson and Ms. A. Thiessen for assistance with the protein expression, and Dr. C. M. Slupsky for help with the smartnotebook program.

REFERENCES

1. Geeves, M. A., and Holmes, K. C. (1999) *Annu. Rev. Biochem. 68*, 687−728.
2. Gordon, A. M., Homsher, E., and Regnier, M. (2000) *Physiol. Rev. 80*, 853−924.
3. Sia, S. K., Li, M. X., Spyracopoulos, L., Gagné, S. M., Liu, W., Putkey, J. A., and Sykes, B. D. (1997) *J. Biol. Chem. 272*, 18216−18221.
4. Dvoretsky, A., Abusamhadneh, E. M., Howarth, J. W., and Rosevear, P. R. (2002) *J. Biol. Chem. 277*, 38565−38570.
5. Spyracopoulos, L., Li, M. X., Sia, S. K., Gagné, S. M., Chandra, M., Solaro, R. J., and Sykes, B. D. (1997) *Biochemistry 36*, 12138−12146.
6. Solaro, R. J., and Rarick, H. M. (1998) *Circ. Res. 83*, 471−480.
7. Vassylyev, D. G., Takeda, S., Wakatsuki, S., Maeda, K., and Maeda, Y. (1998) *Proc. Natl. Acad. Sci. U.S.A. 95*, 4847−4852.
8. Li, M. X., Spyracopoulos, L., and Sykes, B. D. (1999) *Biochemistry 38*, 8289−8298.
9. Lindhout, D. A., and Sykes, B. D. (2003) *J. Biol. Chem. 278*, 27024−27034.
10. Takeda, S., Yamashida, A., Maeda, K., and Maeda, Y. (2003) *Nature 424*, 35−41.
11. Buscemi, N., Foster, D. B., Neverova, I., and Van Eyk, J. E. (2002) *Circ. Res. 91*, 509−516.
12. Redwood, C. S., Moolman-Smook, J. C., and Watkins, H. (1999) *Cardiovasc. Res. 44*, 20−36.
13. Hernandez, O. M., Housmans, P. R., and Potter, J. D. (2001) *J. Appl. Physiol. 90*, 1125−1136.
14. McDonough, J. L., Arrell, D. K., and Van Eyk, J. E. (1999) *Circ. Res. 84*, 9−20.
15. Murphy, A. M., Kogler, H., Georgakopoulos, D., McDonough, J. L., Kass, D. A., Van Eyk, J. E., and Marban, E. (2000) *Science 287*, 488−491.
16. D'Costa, M., Fleming, E., and Patterson, M. C. (1997) *Am. J. Clin. Pathol. 108*, 550−555.
17. Van Eyk, J. E., Powers, F., Law, W., Larue, C., Hodges, R. S., and Solaro, R. J. (1998) *Circ. Res. 82*, 261−271.
18. McDonough, J. L., Labugger, R., Pickett, W., Tse, M. Y., MacKenzie, S., Pang, S. C., Atar, D., Ropchan, G., and Van Eyk, J. E. (2001) *Circulation 103*, 58−64.
19. Lee, T. H., and Goldman, L. (2000) *N. Engl. J. Med. 342*, 1187−1195.
20. Elliott, K., Watkins, H., and Redwood, C. S. (2000) *J. Biol. Chem. 275*, 22069−22074.

21. James, J., Zhang, Y., Osinska, H., Sanbe, A., Klevitsky, R., Hewett, T. E., and Robbins, J. (2000) *Circ. Res. 87*, 805−811.
22. Takahashi-Yanaga, F., Morimoto, S., Harada, K., Minakami, R., Shiraishi, F., Ohta, M., Lu, Q. W., Sasaguri, T., and Ohtsuki, I. (2001) *J. Mol. Cell Cardiol. 33*, 2095−2107.
23. Deng, Y., Schmidtmann, A., Redlich, A., Westerdorf, B., Jaquet, K., and Thieleczek, R. (2001) *Biochemistry 40*, 14593−14602.
24. Lang, R., Gomes, A. V., Zhao, J., Housmans, P. R., Miller, T., and Potter, J. D. (2002) *J. Biol. Chem. 277*, 11670−11678.
25. Burkart, E. M., Sumandea, M. P., Kobayashi, T., Nili, M., Martin, A. F., Homsher, E., and Solaro, R. J. (2003) *J. Biol. Chem. 278*, 11265−11272.
26. Pearlstone, J. R., Chandra, M., Sorenson, M. M., and Smillie, L. B. (2000) *J. Biol. Chem. 275*, 35106−35115.
27. Li, M. X., Saude, E. J., Wang, X., Pearlstone, J. R., Smillie, L. B., and Sykes, B. D. (2002) *Eur. Biophys. J. 31*, 245−256.
28. Chandra, M., Dong, W. J., Pan, B. S., Cheung, H. C., and Solaro, R. J. (1997) *Biochemistry 36*, 13305−13311.
29. Li, M. X., Gagné, S. M., Spyracopoulos, L., Kloks, C. P. A. M., Audette, G., Chandra, M., Solaro, R. J., Smillie, L. B., and Sykes, B. D. (1997) *Biochemistry 36*, 12519−12525.
30. Tripet, B. P., Van Eyk, J. E., and Hodges, R. S. (1997) *J. Mol. Biol. 271*, 728−750.
31. Huth, J. R., Bewley, C. A., Jackson, B. M., Hinnebusch, A. G., Clore, G. M., and Gronenborn, A. M. (1997) *Protein Sci. 6*, 2359−2364.
32. Lindhout, D. A., Li, M. X., Schieve, D., and Sykes, B. D. (2002) *Biochemistry 41*, 7267−74.
33. Kay, L. E., Keifer, P., and Saarinen, T. (1992) *J. Am. Chem. Soc. 114*, 10663−10665.
34. Zhang, O., Kay, L. E., Olivier, J. P., and Forman-Kay, J. D. (1994) *J. Biomol. NMR 4*, 845−858.
35. Delaglio, F., Grzesiek, S., Vuister, G. W., Zhu, G., Pfeifer, J., and Bax, A. (1995) *J. Biomol. NMR 6*, 277−293.
36. Johnson, B. A., and Blevins, R. A. (1994) *J. Biomol. NMR 4*, 603−614.
37. Wang, X., Li, M. X., Spyracopoulos, L., Beier, N., Chandra, M., Solaro, R. J., and Sykes, B. D. (2001) *J. Biol. Chem. 276*, 25456−66.
38. Muhandiram, D. R., and Kay, L. E. (1994) *J. Magn. Reson. B103*, 203−216.
39. Slupsky, C. M., Boyko, R. F., Booth, V. K., and Sykes, B. D. (2003) *J. Biomol. NMR 27*, 313−321.
40. Wang, X., Li, M. X., and Sykes, B. D. (2002) *J. Biol. Chem. 277*, 31124−31133.

BI035408Y